Aerosol and Air Quality Research, 18: 1660–1672, 2018

ISSN: 1680-8584 print / 2071-1409 online
doi: 10.4209/aaqr.2017.08.0259

Source Profiles for $PM_{10-2.5}$ Resuspended Dust and Vehicle Exhaust Emissions in Central India

Shamsh Pervez[1*], Shahina Bano[1], John G. Watson[2,7], Judith C. Chow[2,7], Jeevan Lal Matawle[1,3], Anjali Shrivastava[4], Suresh Tiwari[5], Yasmeen Fatima Pervez[6]**

[1] *School of Studies in Chemistry, Pt. Ravishankar Shukla University, Raipur 492010, Chhattisgarh, India*
[2] *Division of Atmospheric Sciences, Desert Research Institute, Reno, NV 89512, USA*
[3] *Directorate of Geology and Mining, Chhattisgarh, Regional Laboratory, Jagdalpur 494001, Chhattisgarh, India*
[4] *National Environmental Engineering Research Institute, Nagpur 440020, Maharashtra, India*
[5] *Indian Institute of Tropical and Meteorology (IITM), New Delhi 110060, India*
[6] *Department of Engineering Chemistry, Chhatrapati Shivaji Institute of Technology, Durg 491010, Chhattisgarh, India*
[7] *Institute of Earth and Environment, Chinese Academy of Science, Xian 710061, China*

ABSTRACT

Eight composite $PM_{10-2.5}$ source profiles were developed for resuspended dust and vehicle exhaust emissions with 32 chemical species, including 21 elements (Al, As, Ca, Cd, Co, Cr, Cu, Fe, Hg, K, Mg, Mn, Mo, Na, Ni, Pb, S, Sb, Se, V, and Zn), 9 water-soluble ions (Na^+, K^+, Mg^{2+}, Ca^{2+}, NH_4^+, Cl^-, F^-, NO_3^-, and SO_4^{2-}), and carbonaceous fractions (OC and EC). Dust samples were dominated by crustal elements (Al, Ca, Fe, and Mg) while exhaust emissions showed high abundances of carbonaceous aerosol (OC and EC). Crustal species (Al, Fe, Mg, and Na) were more enriched over native soils in $PM_{10-2.5}$ as compared to $PM_{2.5}$. The higher coefficients of divergence (COD) indicate that profiles differ from each other. Ca accounted for nearly 30% of $PM_{10-2.5}$ mass in construction dust while Fe accounted for nearly 20% of $PM_{10-2.5}$ mass in paved road dust. Three- and four-wheeler diesel exhaust profiles consisted of 5–7% EC, with 6–10 times higher Pb, Se, and S abundances than those in two-wheeler gasoline exhaust profile. The heavy-duty diesel exhaust profile consist of nearly 20% EC with abundant (> 0.5%) trace elements (e.g., Pb, Se, and Zn).

Keywords: $PM_{10-2.5}$; Source profile; Enrichment factor; Source markers; Resuspended dust; Vehicle exhaust.

INTRODUCTION

Air pollution is of great concern in India, especially the high levels of particulate matter (PM) emitted from uncontrolled industrial processes, solid waste and biomass burning, vehicular exhaust, and resuspended road dust (Pant and Harrison, 2013; Pant *et al.*, 2015). Real-world source characterizations are needed to obtain chemical source profiles for input to receptor models, such as the Chemical Mass Balance (CMB), to identify and quantify source contributions. The U.S. EPA SPECIATE (USEPA, 2013), European SPECIEUROPE (Pernigotti *et al.*, 2016), and China Source Profile Shared Service (CSPSS) (Liu *et al.*, 2017) databases have assembled many of these profiles.

Gargava and Rajagopalan (2016) found that road dust and vehicular exhaust emissions account for ~30–70% and ~15–20% of the measured PM_{10} mass, respectively, in India. Various studies have been conducted (Chow *et al.*, 2003; Ho *et al.*, 2003; Kong *et al.*, 2011, Patil *et al.*, 2013; Han *et al.*, 2014; Kong *et al.*, 2014; Matawle *et al.*, 2015; Pant *et al.*, 2015; Wang *et al.*, 2015; Liu *et al.*, 2016) to derive dust and motor vehicle exhaust profiles (Chow *et al.*, 2004; Han *et al.*, 2014; Matawle *et al.*, 2015; Liu *et al.*, 2017). This study reports additional $PM_{10-2.5}$ chemical source profiles for resuspended dust and vehicle exhaust emissions specific to India.

METHODOLOGY

Source Sampling and Chemical Analysis

Source sampling was conducted in Raipur, the capital of Chhattisgarh, India (21°14′22.7″N, 81°38.1″E), with a population of ~1.6 million (Census, 2011), as documented by Matawle *et al.* (2014, 2015) for $PM_{2.5}$. This paper describes the $PM_{10-2.5}$ chemical profiles for the eight resuspended dust and vehicle exhaust emissions tests. Source samples are summarized in Table 1. Geological samples typical of Central

[*] Corresponding author: Tel: +91 9425242455
E-mail address: shamshpervez@gmail.com
[**] Corresponding author.
E-mail address: Judy.Chow@dri.edu

Table 1. Descriptions of source type, sampling location, and source sampling method.

Profile Mnemonic	Source type	Description/Location[a]	Source sampling method
SD	Natural Soil Dust	Non-agricultural soil outside the city of Raipur	Chamber resuspension sampling
CD	Civil Construction Dust	Dust samples from a construction site located in the study area	Chamber resuspension sampling
PRD	Paved Road Dust	Dust samples from the surface of paved road of the study area	Chamber resuspension sampling
UPRD	Unpaved Road Dust	Dust samples from the surface of unpaved road outside the city of Raipur	Chamber resuspension sampling
2WVG	Two-Wheeler Vehicles (gasoline)	Samples from exhaust pipes of petrol driven 2-wheelers	In-plume sampling
3WVD	Three-Wheeler Vehicles (diesel)	Samples from exhaust pipes of diesel driven 3-wheelers passenger auto rickshaws	In-plume sampling
4WVD	Four-Wheeler Vehicles (diesel)	Samples from exhaust pipes of diesel driven 4-wheelers personal cars	In-plume sampling
HDVD	Heavy Duty Vehicles	Samples from exhaust pipes of diesel driven heavy duty trucks	In-plume sampling

[a] Five samples were collected and composited to develop each source profile.

India include paved road and construction dust in Raipur City, as well as unpaved surface dust and non-agricultural soils outside of Raipur City. Sweeping and grab sampling methods were employed to obtain 0.5–1 kg of each dust which were air dried (~25°C), sieved (Tyler 400 mesh to 38 µm in geological diameter), and resuspended in a laboratory chamber through $PM_{2.5}$ and PM_{10} inlets at 5 L min^{-1} following Chow *et al.* (1994) as applied in past studies (Watson and Chow, 2001; Watson *et al.*, 2001; Chow *et al.*, 2004).

Motor vehicle exhaust samples were acquired from four major vehicle categories that are common in India including: two-wheeler gasoline, three- and four-wheeler diesel, and heavy-duty diesel vehicles. Vehicles manufactured between 2000 and 2001 were selected for in-plume sampling through collocated $PM_{2.5}$ and PM_{10} inlets on Minivol samplers (Airmetrics) at a flow rate of 5 L min^{-1}. Vehicles were operated under steady state conditions for 30–60 minutes to ensure adequate deposit on quartz-fiber filters (Whatman catalog No. 1851-047) for subsequent chemical analysis. Five sets of samples were collected from each source, for a total of 40 samples.

Quartz-fiber filters were weighed before and after sampling with a ± 10 µg sensitivity digital balance (Denver, Model, TB-2150) (Watson *et al.*, 2017). These samples were analysed for 21 elements (Al, As, Ca, Cd, Co, Cr, Cu, Fe, Hg, K, Mg, Mn, Mo, Na, Ni, Pb, S, Sb, Se, V, Zn) by atomic absorption spectrophotometry; 8 cations and anions (Na^+, K^+, Mg^{2+}, Ca^{2+}, NH_4^+, Cl^-, F^-, NO_3^-, and SO_4^{2-}) by ion chromatography (Chow and Watson, 2017); ammonium (NH_4^+) by spectrophotometry; and organic and elemental carbon (OC and EC) by thermal/optical transmittance.

Detailed chemical analysis and quality assurance/quality control procedures are documented in Matawle *et al.* (2014, 2015). Laboratory filter blanks and field trip blanks were submitted to the same chemical analysis to assess background levels. One standard sample was analysed after each 10 samples to assure 80%–120% recovery. Triplicate analyses were performed for each sample to achieve ±10% reproducibility. The limits of detections (LODs) for each species were reported in Matawle *et al.* (2014).

RESULTS AND DISCUSSION

$PM_{10-2.5}$ Chemical Source Profile

The four resuspended dust and four vehicle exhaust profiles are summarized in Tables 2 and 3, respectively. The sum of species accounted for 40–47% and 52–69% of $PM_{10-2.5}$ mass for dust and vehicle exhaust profiles, respectively. Crustal elements (Al, Ca, Fe, K, Mg, and Na) were the most abundant species in dust, contributing 31–45% of the $PM_{10-2.5}$ mass, whereas total carbon (TC = OC + EC) constituted 49–57% exhaust. The OC/TC ratios ranged from 0.65–0.98, comparable to 0.57–0.98 reported in India for PM_{10} (CPCB, 2008b) and $PM_{2.5}$ (Matawle *et al.*, 2015). The low sum of species for dust is mainly due to the lack of silicon (Si) in the profile. Si is often the most abundant element in crustal dust (Chow *et al.*, 2003). The quartz-fiber filter prohibits Si analysis and the use of Si/Al ratio as

Table 2. $PM_{10-2.5}$ composite sources profiles (weight percent by mass) for resuspended dust inside and outside of Raipur City.

Species	Profile Mnemonic [a]			
	SD	CD	PRD	UPRD
Al	3.374 ± 0.451	2.346 ± 0.871	0.844 ± 0.119	0.906 ± 0.144
As	0.000 ± 0.000	0.000 ± 0.000	0.006 ± 0.005	0.003 ± 0.004
Ca	14.331 ± 2.187	27.859 ± 7.313	18.573 ± 2.607	15.049 ± 3.569
Cd	0.000 ± 0.000	0.001 ± 0.001	0.003 ± 0.003	0.001 ± 0.001
Co	0.001 ± 0.001	0.001 ± 0.001	0.001 ± 0.001	0.001 ± 0.001
Cr	0.040 ± 0.007	0.002 ± 0.001	0.009 ± 0.002	0.003 ± 0.002
Cu	0.103 ± 0.030	0.016 ± 0.007	0.021 ± 0.003	0.013 ± 0.003
Fe	9.014 ± 0.504	7.053 ± 0.705	11.291 ± 0.658	17.457 ± 0.811
Hg	0.000 ± 0.001	0.001 ± 0.003	0.007 ± 0.007	0.008 ± 0.013
K	0.613 ± 0.036	0.151 ± 0.040	0.431 ± 0.067	0.435 ± 0.060
Mg	2.279 ± 0.446	3.715 ± 0.434	2.125 ± 0.151	3.016 ± 0.214
Mn	0.026 ± 0.013	0.152 ± 0.014	0.069 ± 0.012	0.088 ± 0.014
Mo	0.000 ± 0.000	0.002 ± 0.004	0.003 ± 0.001	0.002 ± 0.001
Na	1.726 ± 0.097	3.508 ± 0.209	1.024 ± 0.083	0.649 ± 0.037
Ni	0.015 ± 0.012	0.007 ± 0.005	0.017 ± 0.009	0.007 ± 0.009
Pb	0.001 ± 0.001	0.001 ± 0.000	0.016 ± 0.009	0.004 ± 0.005
S	0.007 ± 0.003	0.004 ± 0.992	0.037 ± 0.730	0.008 ± 0.083
Sb	0.002 ± 0.001	0.001 ± 0.000	0.009 ± 0.005	0.008 ± 0.004
Se	0.000 ± 0.000	0.000 ± 0.000	0.009 ± 0.006	0.013 ± 0.004
V	0.003 ± 0.001	0.006 ± 0.003	0.023 ± 0.004	0.007 ± 0.002
Zn	0.042 ± 0.055	0.134 ± 0.115	0.069 ± 0.005	0.006 ± 0.002
F^-	0.005 ± 0.005	0.001 ± 0.001	0.488 ± 0.036	0.026 ± 0.013
Cl^-	0.961 ± 0.118	0.027 ± 0.008	0.089 ± 0.064	0.099 ± 0.050
NO_3^-	0.649 ± 0.198	0.015 ± 0.008	0.019 ± 0.014	0.025 ± 0.011
SO_4^{2-}	0.847 ± 0.135	0.005 ± 0.005	0.988 ± 0.076	0.324 ± 0.033
Na^+	0.417 ± 0.083	0.001 ± 0.000	0.512 ± 0.152	0.077 ± 0.016
NH_4^+	0.073 ± 0.026	0.014 ± 0.009	0.089 ± 0.064	0.069 ± 0.049
K^+	0.051 ± 0.031	0.010 ± 0.002	0.061 ± 0.059	0.082 ± 0.089
Ca^{2+}	1.943 ± 0.199	0.362 ± 0.095	3.435 ± 0.413	2.416 ± 0.394
Mg^{2+}	0.027 ± 0.002	0.108 ± 0.014	0.532 ± 0.058	0.975 ± 0.046
OC	4.257 ± 8.175	2.214 ± 2.156	5.568 ± 3.528	2.111 ± 1.255
EC	1.908 ± 0.873	0.056 ± 3.049	1.636 ± 0.818	1.629 ± 0.515
TC	6.165 ± 9.048	2.270 ± 5.205	7.204 ± 4.346	3.741 ± 1.770
OC/EC	2.23	39.75	3.40	1.30
OC/TC	0.69	0.98	0.77	0.56
SUM%	40.278 ± 3.376	47.291 ± 4.962	43.467 ± 4.908	41.972 ± 3.112

[a] See profile description in Table 1.

a source marker (Contini *et al.*, 2016). Future studies should be conducted with parallel Teflon-membrane and quartz-fiber filters to accommodate complete chemical speciation (Chow *et al.*, 1994; Watson *et al.*, 2001).

Source Profile for Resuspended Dust

Fig. 1 shows four abundant crustal species: Ca, Fe, Mg, and Al. The most abundant species, Ca, varied two-fold among the four profiles, from 27.9 ± 7.3% in construction dust (CD) to 14.3 ± 22% in non-agricultural soils (SD). Ca is commonly found in construction dust (Yatkin and Bayram, 2008; Kong *et al.*, 2011; Pant and Harrison, 2012; Shen *et al.*, 2016) owing to its presence in concrete. Ca was not water soluble, with Ca^{2+}/Ca values in the range of 0.14–0.18, with a lower ratio for construction dust (0.012). Fe was most abundant (17.5 ± 0.8%) in unpaved road dust (UPRD), compared to a lower abundance in construction dust (CD, 7.1 ± 0.7%). Al levels were low (0.8–0.9%) in paved and unpaved road dust, but they were highest at 2–3% in soil and construction dust. Mg levels were similar, in the range of 2–4% of $PM_{10-2.5}$ mass. These abundances are comparable to those from past studies for $PM_{2.5}$, $PM_{10-2.5}$, and PM_{10} (Chow and Watson, 1994; Watson *et al.*, 2001; Amato *et al.*, 2009; Patil *et al.*, 2013; Matawle *et al.*, 2015; Wang *et al.*, 2015; Samiksha *et al.*, 2017). As expected, most of the soil-related K was not water soluble. K was 12 times higher than soluble K^+ with a K^+/K ratio of 0.08; higher than 0.1–0.5 reported in past PM_{10} (CPCB, 2008a; Kong *et al.*, 2014) and $PM_{2.5}$ (Watson *et al.*, 2001; Matawle *et al.*, 2015) studies. This is in contrast to biomass burning profiles where the K^+/K ratio is in the range of ~0.87–0.90 (Watson *et al.*, 2001; Chow *et al.*, 2004). TC accounted for

Table 3. $PM_{10-2.5}$ composite sources profiles (weight percent by mass) for vehicle exhaust emissions.

Species	Profile Mnemonic[a]			
	2WVG	3WVD	4WVD	HDVD
Al	0.004 ± 0.009	0.007 ± 0.005	0.216 ± 0.175	0.103 ± 0.335
As	0.001 ± 0.000	0.000 ± 0.000	0.000 ± 0.000	0.001 ± 0.001
Ca	0.376 ± 0.483	0.498 ± 0.719	0.075 ± 0.159	0.133 ± 0.168
Cd	0.000 ± 0.000	0.000 ± 0.000	0.001 ± 0.001	0.000 ± 0.000
Co	0.000 ± 0.000	0.000 ± 0.000	0.000 ± 0.000	0.000 ± 0.000
Cr	0.003 ± 0.002	0.001 ± 0.001	0.001 ± 0.001	0.001 ± 0.001
Cu	0.059 ± 0.018	0.017 ± 0.013	0.024 ± 0.011	0.019 ± 0.021
Fe	0.477 ± 0.527	0.749 ± 0.627	0.548 ± 0.306	0.286 ± 0.304
Hg	0.004 ± 0.008	0.001 ± 0.002	0.001 ± 0.001	0.002 ± 0.006
K	0.002 ± 0.002	0.014 ± 0.018	0.014 ± 0.003	0.002 ± 0.003
Mg	0.019 ± 0.018	0.046 ± 0.025	0.046 ± 0.027	0.005 ± 0.003
Mn	0.006 ± 0.005	0.002 ± 0.004	0.003 ± 0.003	0.002 ± 0.002
Mo	0.003 ± 0.003	0.001 ± 0.003	0.001 ± 0.002	0.002 ± 0.002
Na	1.249 ± 1.537	0.629 ± 1.523	1.647 ± 1.694	6.655 ± 5.157
Ni	0.006 ± 0.007	0.002 ± 0.001	0.005 ± 0.004	0.005 ± 0.005
Pb	0.042 ± 0.002	0.310 ± 0.028	0.473 ± 0.029	0.774 ± 0.063
S	0.050 ± 0.293	0.547 ± 0.082	0.579 ± 0.047	0.528 ± 0.139
Sb	0.014 ± 0.001	0.014 ± 0.002	0.013 ± 0.003	0.018 ± 0.002
Se	0.040 ± 0.005	0.260 ± 0.056	0.058 ± 0.014	0.757 ± 0.085
V	0.007 ± 0.004	0.001 ± 0.001	0.001 ± 0.001	0.004 ± 0.003
Zn	0.399 ± 0.346	0.601 ± 0.541	0.567 ± 0.307	0.906 ± 0.314
F^-	0.083 ± 0.018	0.000 ± 0.000	0.000 ± 0.000	0.000 ± 0.000
Cl^-	0.135 ± 0.121	0.563 ± 0.243	0.062 ± 0.034	1.100 ± 0.129
NO_3^-	0.002 ± 0.002	0.004 ± 0.005	0.000 ± 0.000	0.001 ± 0.000
SO_4^{2-}	0.118 ± 0.096	0.805 ± 0.107	0.876 ± 0.105	1.002 ± 0.173
Na^+	0.694 ± 0.282	0.486 ± 0.276	0.307 ± 0.664	0.828 ± 0.482
NH_4^+	0.068 ± 0.019	0.178 ± 0.062	0.069 ± 0.029	0.209 ± 0.011
K^+	0.001 ± 0.001	0.003 ± 0.001	0.005 ± 0.001	0.002 ± 0.001
Ca^{2+}	0.116 ± 0.027	0.316 ± 0.211	0.058 ± 0.019	0.061 ± 0.031
Mg^{2+}	0.005 ± 0.006	0.031 ± 0.036	0.029 ± 0.008	0.003 ± 0.004
OC	48.103 ± 6.589	45.205 ± 2.647	44.537 ± 3.753	37.167 ± 1.887
EC	0.754 ± 0.210	4.621 ± 1.216	7.406 ± 0.497	19.711 ± 1.524
TC	48.857 ± 6.800	49.826 ± 3.864	51.943 ± 4.250	56.878 ± 3.411
OC/EC	63.77	9.78	6.01	1.89
OC/TC	0.98	0.91	0.86	0.65
SUM%	52.026 ± 7.329	55.076 ± 5.935	57.213 ± 7.208	69.396 ± 8.339

[a] See profile description in Table 1.

2–7% of $PM_{10-2.5}$ mass. The OC abundance in PRD was 5.6 ± 3.5% compared to that in UPRD at 2.1 ± 1.3%. Heavily travelled roads are subject to more vehicle exhaust deposition. Pb, V, and S abundances were 3–5 times higher in PRD as compared to other dusts, similar to abundances in other Indian cities for PM_{10} (Samara, 2005; CPCB, 2008a). OC/TC ratios ranged from 0.56 in UPRD to 0.98 in CD, consistent with 0.64–0.99 reported in past PM_{10} studies (Ho *et al.*, 2003; Chow *et al.*, 2004; Gupta *et al.*, 2007).

Enrichment Factors (EF) were calculated relative to Ca in local soil as a reference element because: (1) The study region is located in a rock basin with high Ca abundances; (2) Ca correlates with other elements in the dust matrix (Quraishi, 1997); and (3) Past studies have used Ca as an EF reference element (Sharma and Pervez, 2003). The EF (Cao *et al.*, 2008; Chakraborty and Gupta, 2009; Behera and Sharma, 2010) is:

$$EF = \frac{(X_i / Ca)_{sample}}{(X_i / Ca)_{crust}} \quad (1)$$

where (X_i/Ca)sample and (X_i/Ca) crust are ratios of the abundance of element X_i and Ca in PM samples and in crustal materials, respectively. Fig. 2 shows elemental EFs and Fig. 3 compares EFs for $PM_{10-2.5}$ and $PM_{2.5}$ profiles (Matawle *et al.*, 2015). EFs for both size fractions are detailed in Supplemental Table S1. As shown in Fig. 3, Cd had high EFs for all sources ranging from 9–17 for $PM_{2.5}$ and 2–8 for $PM_{10-2.5}$, comparable to other studies (Han *et al.*, 2014; Kong *et al.*, 2014). For PRD and UPRD profiles, As, Cu, and Zn were enriched (EF > 5 for $PM_{2.5}$ and EF > 3 for $PM_{10-2.5}$), consistent with influences from traffic emissions such as tire and brake wear. Most of the crustal species (Al and Mg) were enriched in $PM_{10-2.5}$ as compared

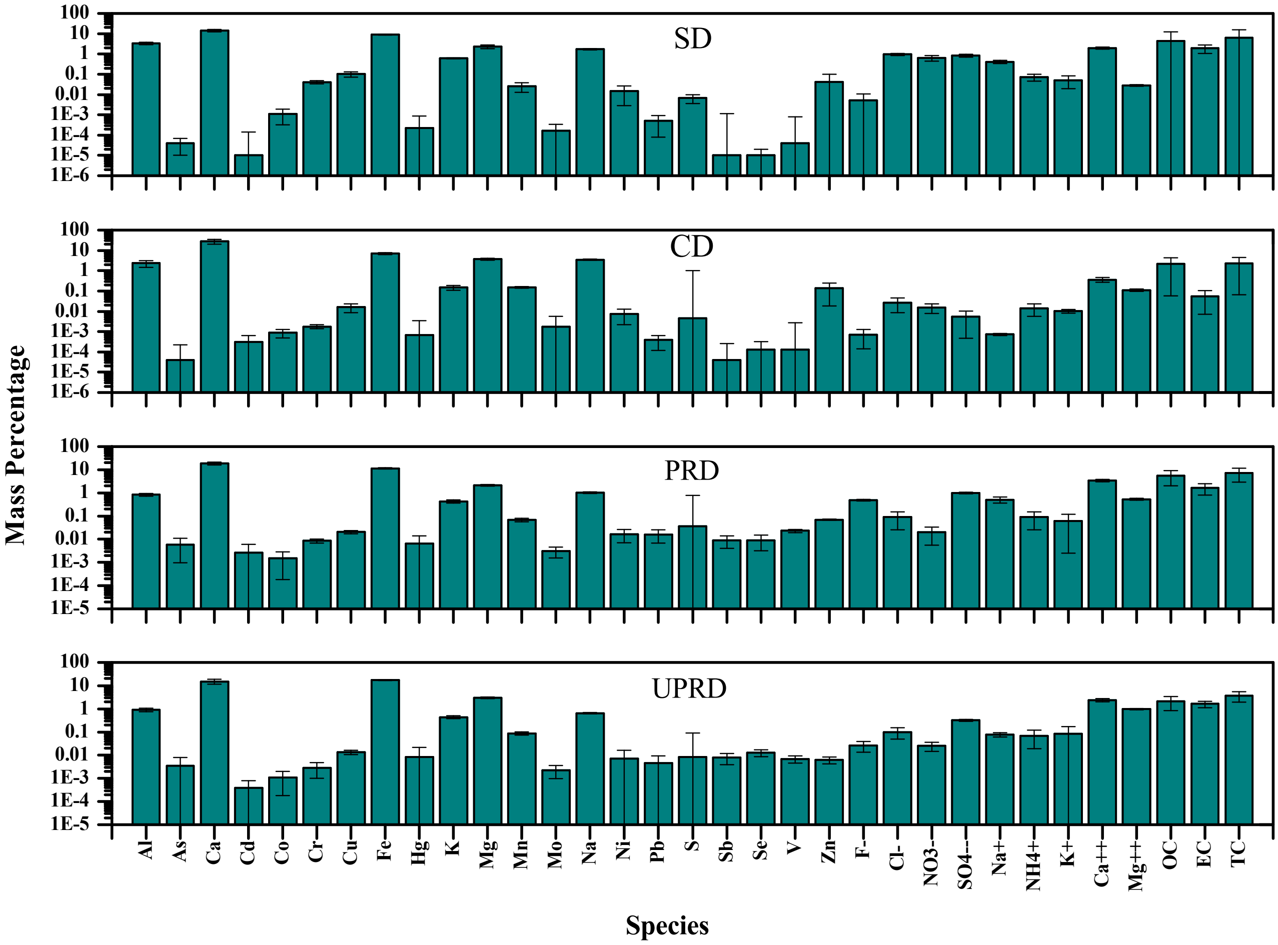

Fig. 1. $PM_{10\text{-}2.5}$ source profiles for non-agriculture soil dust (SD), construction dust (CD), paved road dust (PRD), and unpaved road dust (UPRD)

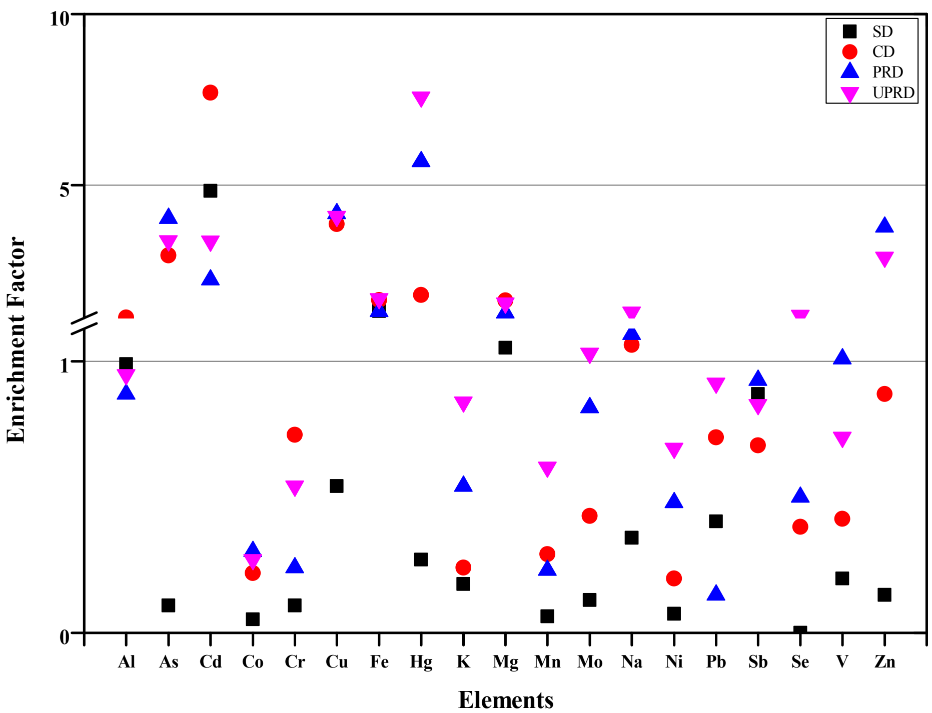

Fig. 2. Enrichment Factors (EF) for elements in $PM_{10\text{-}2.5}$ resuspended dust. Ca was used as the reference element.

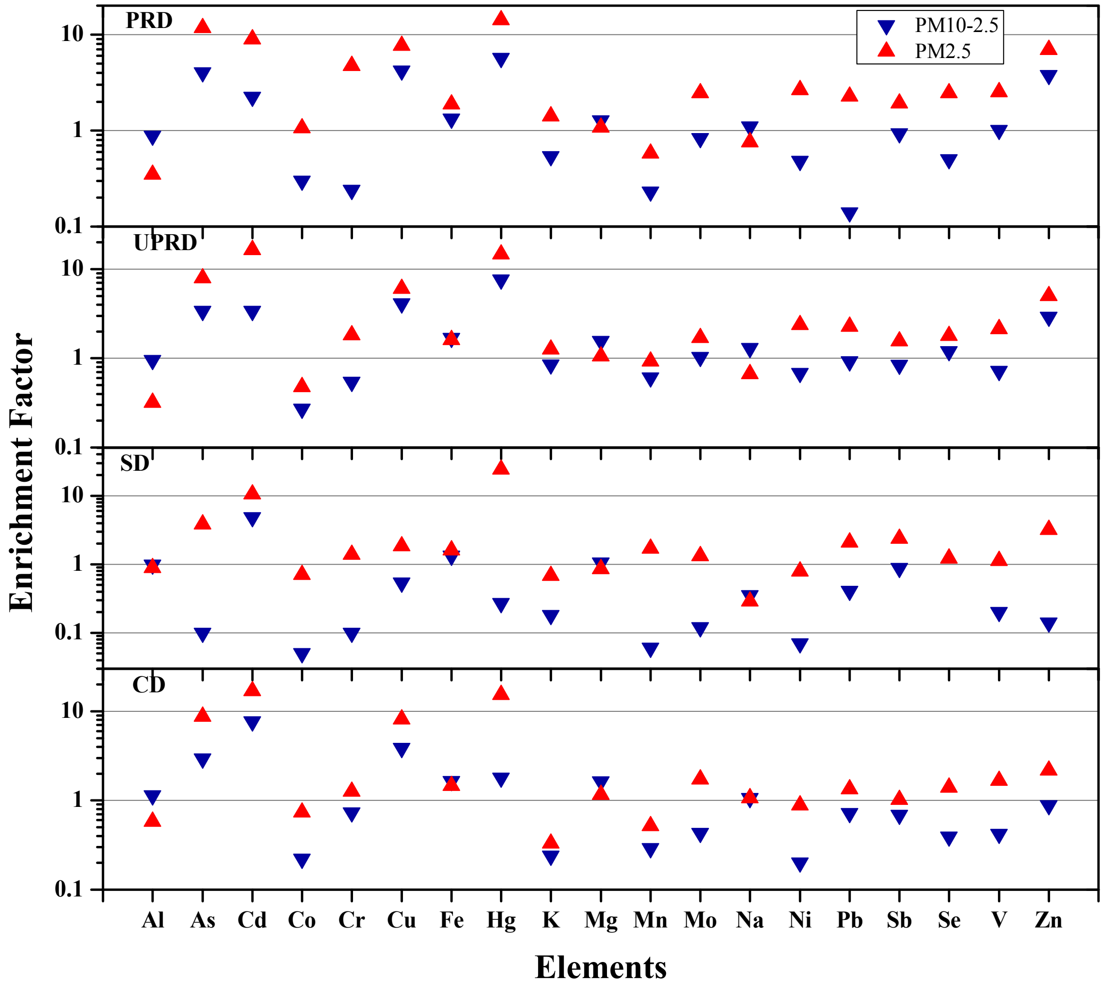

Fig. 3. Enrichment Factors for $PM_{10\text{-}2.5}$ and $PM_{2.5}$ resuspended dust.

to $PM_{2.5}$, while most of the anthropogenic related elements were more abundant in $PM_{2.5}$.

Source Profiles for Vehicle Exhaust Emissions

The four exhaust profiles are shown in Fig. 4. TC was the most abundant species accounting for 49–57% of the measured mass. The OC abundance was highest for the two-wheeler gasoline exhaust (2WVG, 48% ± 6.6%) whereas the EC abundance was highest for the heavy-duty diesel (HDVD, 19.7% ± 1.5%). These levels were 3–26 times higher than two- to four-wheeler exhaust profiles, but comparable to PM_{10} profiles reported by Han *et al.* (2014). The OC/TC ratios in the range of 0.65 to 0.98 were similar to the 0.55–0.95 for the PM_{10} profiles of Han *et al.* (2014) as well as 0.57–0.98 in Matawle *et al.* (2015) and 0.66–0.80 in Watson *et al.* (2001) for $PM_{2.5}$. The largest difference were in the OC/EC ratios, ranging from 1.9 for HDVD to 63.8 for 2WVG, mainly due to the low EC levels (0.8 ± 0.2%) for two-wheeler gasoline exhaust profile. Other elemental abundances were low except for Na, ranging from 0.63 ± 1.5% in 3WVD to 6.7 ± 5.2% in HDVD. The heavy-duty diesel vehicle profile contained the highest Pb (0.77 ± 0.06%), Se (0.76 ± 0.09%), Cl^- (1.1 ± 0.13%), and SO_4^{2-} (1.0 ± 0.2%), abundances. Three- and four-wheeler diesel exhaust profiles consisted of 5–7% of EC, with 6–10 times higher Pb, Se, and S than two-wheeler gasoline vehicles.

Mass Reconstruction

$PM_{10\text{-}2.5}$ mass reconstruction evaluates closure between gravimetric mass and the major chemical constituents (Watson *et al.*, 2012). Fig. 5 shows reconstructed $PM_{10\text{-}2.5}$ in seven categories (Chow *et al.*, 2015; Pei *et al.*, 2016): (1) geological materials derived from a modified IMPROVE equation (Malm *et al.*, 1994), without the inclusion of Si and Ti, where minerals = 2.2Al + 1.63Ca + 2.42Fe; (2) other elements (all elements measured excluding Na, Mg, Al, S, K, Ca, and Fe); (3) sulphate (SO_4^{2-}); (4) other ions (all ions measured excluding SO_4^{2-} and Ca^{2+}); (5) organic matter (OM = OC × 1.8) to account for unmeasured oxygen and hydrogen (Pitchford *et al.*, 2007); (6) EC; and (7) unidentified species calculated by subtracting the sum of categories 1–6 above from 100, which include species that are not measured (such as Si and Ti) or not adequately accounted for (such as oxide forms of other crustal materials or variations in the OM/OC multiplier).

Approximately 91–93% of measured mass was achieved for exhaust profiles, with lower values (65–76%) for the dust profiles, mainly due to the lack of Si and Ti measurements.

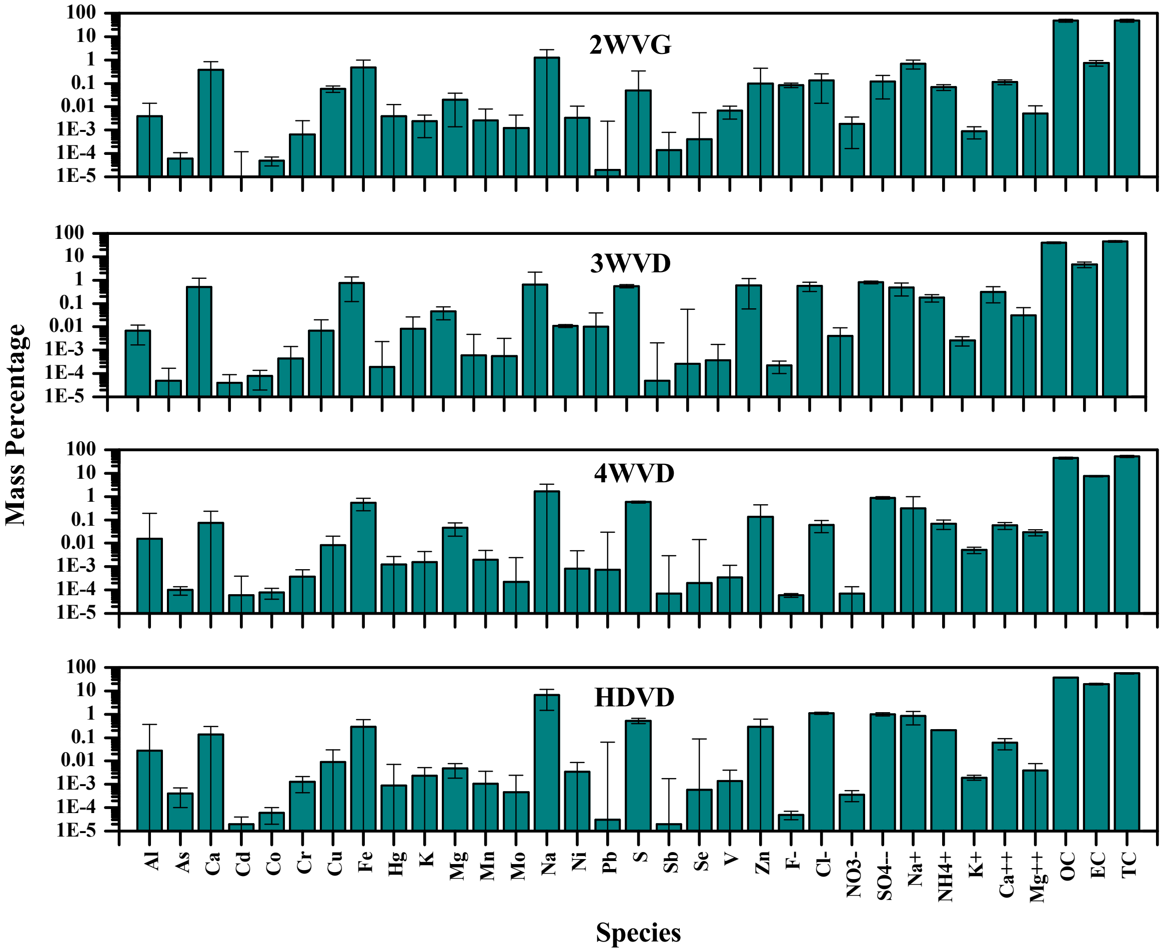

Fig. 4. $PM_{10\text{-}2.5}$ vehicle exhaust profiles for gasoline two-wheeler (2WVG), diesel three- and four-wheelers (3WVD and 4WVD), and heavy-duty diesel (HDVD) vehicles.

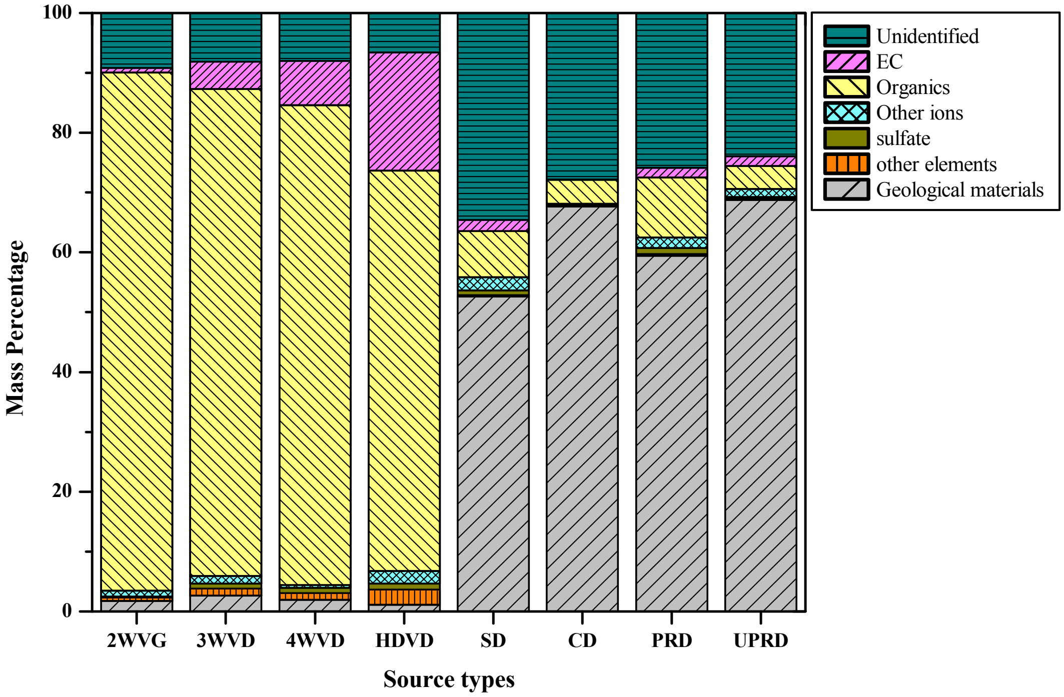

Fig. 5. $PM_{10\text{-}2.5}$ Mass reconstruction for vehicle and resuspended dust sources (See Table 1 for profile Mnemonics).

As expected, OM was the major fraction (72–95%) of exhaust emissions, whereas geological minerals (80–94%) dominated the dust profiles.

Coefficients of Divergence

To evaluate the similarities and differences among the profiles, coefficients of divergence (COD) were calculated, as described by Matawle *et al.* (2014, 2015). When COD values < 0.2, as suggested by Contini *et al.* (2012), the two sources are similar, and when the COD > 0.2 the two sources are considered different (Wongphatarakul *et al.*, 1998; Wilson *et al.*, 200;). Table 4 shows high COD values ranging from 0.48 between 3WVD and 4WVD to 0.84 between PRD and HDVD, indicating that the profiles are not collinear.

Implications for Source Apportionment

Source Markers

Potential source markers are identified by the following equation (Yang *et al.*, 2002; Kong *et al.*, 2011):

$$Ratio_{j,i} = \frac{\left(X_i / \sum X\right)_j}{\left(X_i / \sum X\right)_{min}} \quad (2)$$

where X_i is the i[th] species concentration; $(X_i/\sum X)_j$ is the abundance of i[th] species divided by the sum of the measured 32 species concentration ($\sum X$) for source j; $(X_i/\sum X)_{min}$ is the minimum abundance of the i[th] individual species divided by $\sum X$ (Yang *et al.*, 2002; Chen *et al.*, 2003). Individual species concentrations are further normalized by dividing the i[th] species concentration by the sum of the i[th] concentrations (Kong *et al.*, 2011). Species with the six highest ratios are potential source markers. Similar approaches used by other studies are summarized in Table 5. Past studies (Mitra *et al.*, 2002; Watson *et al.*, 2008; Viana *et al.*, 2008; Guttikunda, 2009; Kong *et al.*, 2011; Matawle *et al.*, 2015) showed that Al, Si, K, Ca, Mg, and Fe were commonly used as markers for dust sources, whereas OC, EC, S, or SO_4^{2-}, and Pb were markers for exhaust. As shown in Table 5, Pb and Se may be markers for paved road dust in $PM_{10\text{-}2.5}$ and for unpaved road dust in $PM_{2.5}$ (Matawle *et al.*, 2015).

Diagnostic Ratios

Diagnostic ratios are used to distinguish among sources (Arditsoglou and Samara, 2005; Kong *et al.*, 2011; Matawle *et al.*, 2015). The V/Ni ratio was used to assess emissions from marine vessels and residual oil combustion and Cu/Sb and Cu/Zn ratios were used for traffic emissions (Pey *et al.*, 2010). Arditsoglou and Samara (2005) used Zn/Pb ratios in the range of 0.3–0.4 as to infer exhaust emissions, and 1.2 for oil combustion. Mitra *et al.* (2002) suggested a Mn/V ratio << 1 for oil burning and >> 1 for coal burning emissions.

Nine elemental ratios (Mn/V, Cu/Sb, As/V, V/Ni, Zn/Pb, Zn/Cd, Cu/Zn, Cu/Cd, and Cu/Pb) are compared with previous studies in Table 6. The Mn/V ratios for dust profiles ranged from 2.98–24.8, mainly due to elevated Mn (2.1–3.7%) and low V (0.003–0.007%) abundances. Mn/V ratios (0.56–1.86) in exhaust profiles were higher than in past studies (0.05–0.74) due to lower V abundances (0.001–0.006%) in $PM_{10\text{-}2.5}$. The Cu/Sb ratios varied from low (1.08–4.2) for exhaust profiles, to high (1.68–48.3) for dust profiles, similar to past PM_{10} studies (CPCB, 2008a; b). The V/Ni ratios (0.28–1.08) for exhaust were comparable to 0.11–0.85 found in the corresponding $PM_{2.5}$ fractions (Matawle *et al.*, 2015), but five times higher than in other studies (Lee *et al.*, 2000; Samara *et al.*, 2003; Moreno *et al.*, 2006; Kong *et al.*, 2011). High Zn/Pb and Zn/Cd ratios in dust profiles suggest a Zn enrichment due to deposition of vehicle exhaust and tire/brake wear.

CONCLUSION

$PM_{10\text{-}2.5}$ source profiles from paved road and construction dust in Raipur, unpaved road dust and non-agricultural soil outside of Raipur, along with vehicle exhaust from gasoline two-wheelers, diesel three- and four-wheeler and heavy-duty diesel vehicles were acquired. In addition to gravimetric mass, these samples were analysed for 21 elemental species, 9 water soluble ions, and carbon (OC and EC). Crustal elements (Al, Ca, Fe and, Mg) dominated the resuspended dust while carbonaceous species (OC and EC) were more abundant in vehicle exhaust emissions. Ca was most abundant in construction dust (27.9 ± 7.3% of $PM_{10\text{-}2.5}$ mass) while the most abundant Fe (17.5 ± 0.8%) was found in unpaved road dust. Heavy-dusty diesel vehicles (HDVD) reported the highest EC abundance (19.7 ± 1.5%) with very low EC (0.75 ± 0.21%) found in gasoline two wheelers (2WVG). Elevated levels of Pb (0.77 ± 0.06%), Se (0.76 ± 0.09%), and Zn (0.91 ± 0.31%) were also apparent in HDVD. The coefficients of divergence (COD) ranged 0.48 to 0.84 suggesting profiles were significantly different

Table 4. Coefficients of Divergence (COD) for resuspended dust and vehicle exhaust emissions

Profile Mnemonic[a]	SD	CD	PRD	UPRD	2WVG	3WVD	4WVD	HDVD
SD	0.00							
CD	0.64	0.00						
PRD	0.64	0.68	0.00					
UPRD	0.56	0.68	0.54	0.00				
2WVG	0.78	0.78	0.76	0.76	0.00			
3WVD	0.73	0.74	0.79	0.73	0.57	0.00		
4WVD	0.75	0.73	0.82	0.75	0.57	0.48	0.00	
HDVD	0.79	0.80	0.84	0.78	0.55	0.53	0.49	0.00

[a] See profile description in Table 1.

Table 5. Source markers of $PM_{10-2.5}$ for resuspended dust and vehicle exhaust emissions.

Aerosol fraction	Source Signatures	References
Resuspended Dust Sources		
1. Soil Dust (SD)		
$PM_{10-2.5}$	***Al, K, Fe, Ca, NO_3^-, and SO_4^{2-}***	**Present study**
$PM_{2.5}$	*Na^+, SO_4^{2-}, Zn, Se, K^+, and Cl^-*	Matawle *et al.*, 2015
PM_{10}	S, NO_3^-, NH_4^+, Zn, Ni, and K^+	Kong *et al.*, 2011
PM	Al, Si, Sc, Ti, Fe, Sm, and Ca	Guttikunda, 2009
2. Construction Dust (CD)		
$PM_{10-2.5}$	***Al, Ca, Mg, NO_3^-, K, and Mg^{2+}***	**Present study**
$PM_{2.5}$	*Zn, Na, Mo, Al, Mg^{2+}, and Ca*	Matawle *et al.*, 2015
PM_{10}	Zn, Mg, V, Mg^{2+}, As, and NO_3^-	Kong *et al.*, 2011
$PM_{2.5}$	Al, Si, K, Ca, and Fe	Watson *et al.*, 2008
3. Paved Road Dust (PRD)		
$PM_{10-2.5}$	**Pb, Mg, Se, NO_3^-, Ca, and K**	**Present study**
$PM_{2.5}$	*Na^+, SO_4^{2-}, As, F^-, Mg^{2+},and Se*	Matawle *et al.*, 2015
PM_{10}	S, Zn, NO_3^-, Cl^-, Mg^{2+}, and NH_4^+	Kong *et al.*, 2011
PM	Ca, Al, Sc, Si, Ti, Fe, and Sm	Guttikunda, 2009
$PM_{2.5}$	Al, Si, K, Ca, and Fe	Watson *et al.*, 2008
4. Unpaved Road Dust (UPRD)		
$PM_{10-2.5}$	**Mg, Mg^{2+}, NO_3^-, K, Al, and Fe**	**Present study**
$PM_{2.5}$	*Na^+, SO_4^{2-}, F^-, Mg^{2+}, Se, and Pb*	Matawle *et al.*, 2015
PM	Ca, Al, Sc, Si, Ti, Fe, and Sm	Guttikunda, 2009
$PM_{2.5}$	Al, Si, K, Ca, and Fe	Watson *et al.*, 2008
Vehicle Exhaust Emissions		
5. Two-Wheeler Vehicles (gasoline) (2WVG)		
$PM_{10-2.5}$	**OC, EC, S, NO_3^-, Cu, and V**	**Present study**
$PM_{2.5}$	F^-, Cr, Cd, V, Na^+, and Ni	Matawle *et al.*, 2015
PM	EC, Br, Ce, La, Pt, SO_4^{2-}, and NO_3^-	Guttikunda, 2009
PM_{10}	Carbon, Fe, Ba, Zn, Cu, and Pb	Vianna *et al.*, 2008
$PM_{2.5}$	OC, EC, NH_3, S, Fe, and Zn	Watson *et al.*, 2008
PM	Br, Pb, and Ba	Mitra *et al.*, 2002
6. *Three-Wheeler Vehicles (diesel) (3WVD)*		
$PM_{10-2.5}$	**Pb, S, EC, SO_4^{2-}, OC, and NH_4^+**	**Present study**
$PM_{2.5}$	Ca^{2+}, Mg^{2+}, NH_4^+, K, Se, and SO_4^{2-}	Matawle *et al.*, 2015
PM	OC, EC, S, SO_4^{2-}, and NO_3^-	Guttikunda, 2009
PM_{10}	Carbon, Fe, Ba, Zn, Cu, and Pb	Vianna *et al.*, 2008
$PM_{2.5}$	OC, EC, NH_3, S, Fe, and Zn	Watson *et al.*, 2008
PM	Br, Pb, and Ba	Mitra *et al.*, 2002
7. Four-Wheeler Vehicles (diesel) (4WVD)		
$PM_{10-2.5}$	**S, EC, OC, SO_4^{2-}, Pb, and Zn**	**Present study**
$PM_{2.5}$	F^-, NO_3^-, Cd, Pb, SO_4^{2-}, and EC	Matawle *et al.*, 2015
PM	OC, EC, S, SO_4^{2-}, and NO_3^-	Guttikunda, 2009
PM_{10}	Carbon, Fe, Ba, Zn, Cu, and Pb	Vianna *et al.*, 2008
$PM_{2.5}$	OC, EC, NH_3, S, Fe, and Zn	Watson *et al.*, 2008
PM	Br, Pb, and Ba	Mitra *et al.*, 2002
8. Heavy Duty Vehicles (diesel) (HDVD)		
$PM_{10-2.5}$	**EC, S, SO_4^{2-}, OC, NH_4^+, and Se**	**Present study**
$PM_{2.5}$	F^-, NH_4^+, Se, Pb, SO_4^{2-}, and EC	Matawle *et al.*, 2015
PM	OC, EC, S, SO_4^{2-}, and NO_3^-	Guttikunda, 2009
PM_{10}	Carbon, Fe, Ba, Zn, Cu, and Pb	Vianna *et al.*, 2008
$PM_{2.5}$	OC, EC, NH_3, S, Fe, and Zn	Watson *et al.*, 2008
PM	Br, Pb, and Ba	Mitra *et al.*, 2002

from each other. Lower than usual mass reconstruction for resuspended dust (65–76%) reconfirm the importance to include Si and Ti in future studies. Source markers were identified as Al, Ca, and Fe for resuspended dust and OC, EC, and Pb for vehicle exhaust emissions. These region-specific profiles are more representative of pollution source characteristics and can be used for future source apportionment studies.

Table 6. Comparison of diagnostic ratios for different source profiles

Source Types	Diagnostic Ratio								
	Mn/V	Cu/Sb	As/V	V/Ni	Zn/Pb	Zn/Cd	Cu/Zn	Cu/Cd	Cu/Pb
This study ($PM_{10-2.5}$)									
SD	8.40	48.25	0.01	0.21	84.25	384.33	2.43	934.26	204.80
CD	24.84	24.85	0.01	0.81	356.69	434.28	0.12	51.64	42.42
PRD	2.98	2.28	0.26	1.39	4.39	26.54	0.29	7.83	1.30
UPRD	12.66	1.68	0.50	0.99	1.38	15.92	2.16	34.40	2.99
2WVG	0.82	4.19	0.04	1.08	9.42	3380.18	0.15	503.50	1.40
3WVD	1.26	1.16	0.12	0.80	1.94	10011.33	0.03	278.90	0.05
4WVD	1.86	1.82	0.10	0.28	1.20	2407.64	0.04	101.22	0.05
HDVD	0.56	1.08	0.11	0.80	1.17	53312.94	0.02	1121.53	0.02
Compiled from National studies									
Matawle *et al.*, 2015 ($PM_{2.5}$)									
Soil	56.51	2.31	0.11	0.93	310.81	3418.93	0.15	524.53	47.68
CD	149.46	1.06	0.07	0.78	1537.17	1566.73	0.03	45.69	44.83
PRD	56.42	1.93	5.48	0.33	3.98	95.58	0.04	4.21	0.18
UPRD	19.75	1.01	1.19	0.82	114.22	670.45	0.02	16.16	2.75
2WVG	0.53	60.51	0.03	0.11	10.04	5127.08	0.36	1865.75	3.65
3WVD	0.15	35.16	0.01	0.73	0.67	3171.63	0.1	320.88	0.07
4WVD	0.08	2.02	0.01	0.62	0.16	326.46	0.29	95.5	0.05
HDVD	0.18	1.34	0.03	0.85	0.01	393.0	1.84	723.5	0.02
Other Studies									
PM_{10} Size Fractions									
Soil[h]	7.17–114.57	0.62–7.96	0.51–3.82	0.12–1.17	0.74–3.66	7.42–69.18	0.08–0.38	2.85–24.39	0.26–0.95
Paved Road Dust[h]	7.32–141.17	0.73–21.76	0.25–3.91	0.04–1.38	0.97–4.94	18.94–144.83	0.05–0.60	7.56–70.36	0.25–2.55
Unpaved Road Dust[h]	8.49–80.38	0.48–26.70	0.43–5.10	0.19–0.49	1.81–4.18	10.97–67.76	0.08–1.34	2.69–32.32	0.19–2.42
Construction[h]	15.22	0.33	1.95	0.41	4.10	115.29	0.02	2.89	0.10
$PM_{2.5}$ Size Fractions									
[1](Comp-2S2WG-all)[i]	0.28	0.07	0.00	-	7.81	-	0.02	-	0.17
[2](Comp-3WD-2)[i]	0.74	0.13	-	3.82	-	-	-	-	0.96
[3](Comp-LCVD-all)[i]	0.05	1.82	0.08	9.11	108.84	26.65	0.01	0.14	0.59
[4](Comp-HCVD-all)[i]	-	0.33	-	-	6.70	2.77	0.09	0.25	0.61
Compiled from International studies									
$PM_{10-2.5}$ Size Fractions									
Road Dust[f]	-	8.54	-	-	-	-	-	-	-
Road Dust[g]	4.87	4.32	0.10	0.94	3.32	227.16	0.20	34.00	0.66
Soil[g]	6.92	1.86	0.08	6.77	2.30	44.22	0.25	7.84	0.50
PM_{10} Size Fractions									
Soil[b]	62.40	-	-	0.77	9.10	344.20	-	-	-
Gasoline vehicles[c]	-	315.00	1.10	0.02	3.40	56.00	-	-	-
Diesel vehicles[c]	-	700.00	0.007	0.15	7.60	407.00	-	-	-
Cement Plant[b]	27.10	-	-	-	21.90	74.50	-	-	-
Cement Plant[c]	-	7.40	0.03	11.00	42.0	195.00	-	-	-
Oil Burning[c]	-	71.00	0.02	4.00	1.20	190.00	-	-	-
Road dust[b,i]	50.60	-	-	0.60	8.50	200.70	-	-	-
Construction dust[b]	37.80	-	-	0.57	11.30	68.10	-	-	-
$PM_{2.5}$ Size Fraction									
Coal Combustion[a]	-	0.50	4.80	0.70	1.90	17.00	-	-	-
Soil[a]	6.30	0.30	0.10	8.30	3.00	9.41	0.30	2.80	0.90
Gasoline + Diesel[a]	-	0.40	-	-	1.70	0.90	0.30	0.30	0.60
Oil burning[d]	-	-	-	2.00	-	-	-	-	-
Traffic[e]	-	3.00–5.00	-	-	-	-	0.10–1.80	200–600	1.20–3.50

[a] Watson *et al.*, 2001; [b] Kong *et al.*, 2011; [c] Samara *et al.*, 2003; [d] Lee *et al.*, 2000; [e] Weckwerth, 2001; [f] Han *et al.*, 2011; [g] Chow *et al.*, 2004; [h] CPCB, 2008a; [I] CPCB, 2008b.
[1] 2-wheeler vehicle-gasoline based (Composite).
[2] 3-wheeler vehicle-diesel based (Composite).
[3] 4-wheeler vehicle-diesel based (Composite).
[4] Heavy-duty vehicle-diesel based (Composite).

ACKNOWLEDGEMENTS

This study was primarily supported by the Department of Science and Technology (India) project SR/S4/AS-61/2010 along with project EMR/2015/000928 and partially supported by the DST-FIST (SR/FST/CSI-259/2014 (c)) and UGC-SAP-DRS-II programs (F-540/7/DRS-II/2016 (SAP-I)). Shahina Bano was supported by a UGC Maulana Azad National Fellowship (F1-17.1/2014-15/MANF-2014-15-MUS-CHH-48224/(SAIII/ Website). The Pt. Ravishankar Shukla University and Indian Institute of Tropical Meteorology (Delhi) provided access to library and laboratory facilities.

SUPPLEMENTARY MATERIAL

Supplementary data associated with this article can be found in the online version at http://www.aaqr.org.

REFERENCES

Amato, F., Pandolfi, M., Escrig, A., Querol, X., Alastuey, A., Pey, J., Perez, N. and Hopke, P.K. (2009). Quantifying road dust resuspension in urban environment by multilinear engine: A comparison with PMF2. *Atmos. Environ.* 43: 2770–2780.

Arditsoglou, A. and Samara, C. (2005). Levels of total suspended particulate matter and major trace elements in Kosovo: A source identification and apportionment study. *Chemosphere* 59: 669–678.

Behera, S.N. and Sharma, M. (2010). Reconstructing primary and secondary components of $PM_{2.5}$ composition for an urban atmosphere. *Aerosol Sci. Technol.* 44: 983–992.

Cao, J.J., Chow, J.C., Watson, J.G., Wu, F., Han, Y.M., Jin, Z.D., Shen, Z.X. and An, Z.S. (2008). Size-differentiated source profiles for fugitive dust in the Chinese Loess Plateau. *Atmos. Environ.* 42: 2261–2275.

Census (2011). Office of the registrar general and census commissioner, India. http://www.censusindia.gov.in/2011

Chakraborty, A. and Gupta, T. (2009). Chemical characterization of submicron aerosol in Kanpur region: A source apportionment study. *Int. J. Environ. Chem. Ecol. Geol. Geophys. Eng.* 3: 56–59.

Chen, S.J., Hsieh, L.T. and Chiu, S.C. (2003). Emission of polycyclic aromatic hydrocarbons from animal carcass incinerators. *Sci. Total Environ.* 313: 61–76.

Chow, J.C. and Watson, J.G. (1994). Contemporary source profiles for geological material and motor vehicle emissions. Report no. DRI 2625.

Chow, J.C., Watson, J.G., Houck, J.E., Pritchett, L.C., Rogers, C.F., Frazier, C.A., Egami, R.T. and Ball, B.M. (1994). A laboratory resuspension chamber to measure fugitive dust size distributions and chemical compositions. *Atmos. Environ.* 28: 3463–3481.

Chow, J.C., Watson, J.G., Ashbaugh, L.L. and Magliano, K.L. (2003). Similarities and differences in PM_{10} chemical source profiles for geological dust from the San Joaquin Valley, California. *Atmos. Environ.* 37: 1317–1340.

Chow, J.C., Watson, J.G., Kuhns, H., Etyemezian, V., Lowenthal, D.H., Crow, D., Kohl, S.D., Engelbrecht, J.P. and Green, M.C. (2004). Source profiles for industrial, mobile, and area sources in the Big Bend Regional Aerosol Visibility and Observational study. *Chemosphere* 54: 185–208.

Chow, J.C., Lowenthal, D.H., Chen, L.W.A., Wang, X. and Watson, J.G. (2015). Mass reconstruction methods for $PM_{2.5}$: A review. *Air Qual. Atmos. Health* 8: 243–263.

Chow, J.C. and Watson, J.G. (2017). Enhanced ion chromatographic speciation of water-soluble $PM_{2.5}$ to improve aerosol source apportionment. *Aerosol Sci. Eng.* 1: 7–24.

Contini, D., Belosi, F., Gambaro, A., Cesari, D., Stortini, A.M. and Bove, M.C. (2012). Comparison of PM_{10} concentrations and metal content in three different sites of the Venice Lagoon: An analysis of possible aerosol sources. *J. Environ. Sci.* 24: 1954–1965.

Contini, D., Cesari, D., Conte, M. and Donateo, A. (2016). Application of PMF and CMB receptor models for the evaluation of the contribution of a large coal-fired power plant to PM_{10} concentrations. *Sci. Total Environ.* 560: 131–140.

CPCB (2008a). Stationary Sources Emission Profiles, Central Pollution Control Board, Delhi. Available from http://www.cpcb.nic.in/Stationary_Sources_Emission_Profiles.xls.

CPCB (2008b). Vehicular Sources Emission Profiles. Central Pollution Control Board, New Delhi, India. http://cpcb.nic.in/Vehicular_Sources_Emission_Profiles.xls, Last Access: 09 October 2014.

Gargava, P. and Rajagopalan, V. (2016). Source apportionment studies in six Indian cities—drawing broad inferences for urban PM_{10} reductions. *Air Qual. Atmos. Health* 5: 471–481.

Gupta, A.K., Karar, K. and Srivastava, A. (2007). Chemical mass balance source apportionment of PM_{10} and TSP in residential and industrial sites of an urban region of Kolkata, India. *J. Hazard. Mater.* 142: 279–287.

Guttikunda, S.K. (2009). *Urban particulate pollution source apportionment: Part 1—Definition, methodology, and resources.* Simple Interactive Models for Better Air Quality: SIM-air Working Paper Series, 016-2009.

Han, J., Han, B., Li, P., Kong, S., Bai, Z., Han, D., Dou, X. and Zhao, X. (2014). Chemical characterizations of PM_{10} profiles for major emission Sources in Xining, Northwestern China. *Aerosol Air Qual. Res*. 14: 1017–1027.

Han, S., Youn, J.S. and Jung, Y.W. (2011). Characterization of PM_{10} and $PM_{2.5}$ source profiles for resuspended road dust collected using mobile sampling methodology. *Atmos. Environ.* 45: 3343–3351.

Ho, K.F., Lee, S.C., Chow, J.C. and Watson, J.G. (2003). Characterization of PM_{10} and $PM_{2.5}$ source profiles for fugitive dust in Hong Kong. *Atmos. Environ.* 37: 1023–1032.

Kong, S., Ji, Y., Lu, B., Chen, L., Han, B., Li, Z. and Bai, Z. (2011). Characterization of PM_{10} source profiles for fugitive dust in Fushun-A city famous for coal. *Atmos. Environ.* 45: 5351–5365.

Kong, S., Ji, Y., Lu, B., Zhao, X., Han, B. and Bai, Z. (2014). Similarities and differences in $PM_{2.5}$, PM_{10} and TSP chemical profiles of fugitive dust sources in a coastal oilfield city in China. *Aerosol Air Qual. Res.* 14:

2017–2028.

Lee, S.W., Pomalis, R. and Kan, B. (2000). A new methodology for source characterization of oil combustion particulate matter. *Fuel Process. Technol.* 65: 189–202.

Liu, Y., Zhang, W., Bai, Z., Yang, W., Zhao, X., Han, B. and Wang, X. (2017). China Source Profile Shared Service (CSPSS): The Chinese $PM_{2.5}$ database for source profiles. *Aerosol Air Qual. Res.* 17: 1401–1414.

Liu, Y., Zhang, W., Bai, Z., Yang, W., Zhao, X., Han, B. and Wang, X. (2016). Characteristics of PM_{10} chemical source profiles for geological dust from the south-west region of China. *Atmosphere* 7: 146.

Malm, W.C., Sisler, J.F., Huffman, D., Eldred, R.A. and Cahill, T.A. (1994). Spatial and seasonal trends in particle concentration and optical extinction in the United States. *J. Geophys. Res. Atmos.* 99: 1347–1370.

Matawle, J., Pervez, S., Dewangan, S., Tiwari, S., Bisht, D.S. and Pervez, Y.F. (2014). $PM_{2.5}$ chemical source profiles of emissions resulting from industrial and domestic burning activities in India. *Aerosol Air Qual. Res.* 14: 2051–2066.

Matawle, J.L., Pervez, S., Dewangan, S., Shrivastava, A., Tiwari, S., Pant, P., Deb, M.K. and Pervez, Y. (2015). Characterization of $PM_{2.5}$ source profiles for traffic and dust sources in Raipur, India. *Aerosol Air Qual. Res.* 15: 2537–2548.

Mitra, A.P., Morawska, L., Sharma, C. and Zhang, J. (2002). Chapter two: Methodologies for characterisation of combustion sources and for quantification of their emissions. *Chemosphere* 49: 903–922.

Moreno, T., Querol, X., Castillo, S., Alastuey, A., Cuevas, E., Herrmann, L., Mounkaila, M., Elvira, J. and Gibbons, W. (2006). Geochemical variations in aeolian mineral particles from the Sahara–Sahel dust corridor. *Chemosphere* 65: 261–270.

Pant, P. and Harrison, R.M. (2012). Critical review of receptor modelling for particulate matter: A case study of India. *Atmos. Environ.* 49: 1–12.

Pant, P. and Harrison, R.M. (2013). Estimation of the contribution of road traffic emissions to particulate matter concentrations from field measurements: A review. *Atmos. Environ.* 77: 78–97.

Pant, P., Baker, S.J., Shukla, A., Maikawa, C., Pollitt, K.J.G. and Harrison, R.M. (2015). The PM_{10} fraction of road dust in the UK and India: Characterization, source profiles and oxidative potential. *Sci. Total Environ.* 530: 445–452.

Patil, R.S., Kumar, R., Menon, R., Shah, M.K. and Sethi, V. (2013). Development of particulate matter speciation profiles for major sources in six cities in India. *Atmos. Res.* 132: 1–11.

Pei, B., Wang, X., Zhang, Y., Hu, M., Sun, Y., Deng, J., Dong, L., Fu, Q. and Yan, N. (2016). Emissions and source profiles of $PM_{2.5}$ for coal-fired boilers in the Shanghai megacity, China. *Atmos. Pollut. Res.* 7: 577–584.

Pernigotti, D., Belis, C.A. and Spanò, L. (2016). SPECIEUROPE: The European data base for PM source profiles. *Atmos. Pollut. Res.* 7: 307–314.

Pey, J., Querol, X. and Alastuey, A. (2010). Discriminating the regional and urban contributions in the North-Western Mediterranean: PM levels and composition. *Atmos. Environ.* 44: 1587–1596.

Pitchford, M., Malm, W., Schichtel, B., Kumar, N., Lowenthal, D. and Hand, J. (2007). Revised algorithm for estimating light extinction from IMPROVE particle speciation data. *J. Air Waste Manage. Assoc*. 57: 1326–1336.

Quraishi, Y.F. (1997). *Study of physico-chemical characteristics of fugitive dusts in relation to respiratory ailments.* Ph. D. Thesis, Pt. Ravishankar Shukla University, Raipur, India.

Samara, C. (2005). Chemical mass balance source apportionment of TSP in a lignite-burning area of Western Macedonia, Greece. *Atmos. Environ.* 39: 6430–6443.

Samara, C., Kouimtzis, T., Tsitouridou, R., Kanias, G. and Simeonov, V. (2003). Chemical mass balance source apportionment of PM_{10} in an industrialized urban area of Northern Greece. *Atmos. Environ.* 37: 41–54.

Samiksha, S., Raman, R.S., Nirmalkar, J., Kumar, S. and Sirvaiya, R. (2017). PM_{10} and $PM_{2.5}$ chemical source profiles with optical attenuation and health risk indicators of paved and unpaved road dust in Bhopal, India. *Environ. Pollut.* 222: 477–485.

Sharma, R. and Pervez, S. (2003). Enrichment and exposure of particulate lead in a traffic environment in India. *Environ. Geochem. Health* 25: 297–306.

Shen, Z., Sun, J., Cao, J., Zhang, L., Zhang, Q., Lei, Y., Gao, J., Huang, R.J., Liu, S. and Huang, Y. (2016). Chemical profiles of urban fugitive dust $PM_{2.5}$ samples in Northern Chinese cities. *Sci. Total Environ.* 569: 619–626.

USEPA (2013). PM composite profiles by source category. http://cfpub.epa.gov/si/speciate/ehpa_speciate_browse.cfm.

Viana, M., Kuhlbusch, T.A.J., Querol, X., Alastuey, A., Harrison, R.M., Hopke, P.K., Winiwarter, W., Vallius, M., Szidat, S. and Prévôt, A.S.H. (2008). Source apportionment of particulate matter in Europe: A review of methods and results. *J. Aerosol Sci.* 39: 827–849.

Wang, X., Chow, J.C., Kohl, S.D., Percy, K.E., Legge, A.H. and Watson, J.G. (2015). Characterization of $PM_{2.5}$ and PM_{10} fugitive dust source profiles in the Athabasca Oil Sands Region. *J. Air Waste Manage. Assoc.* 65: 1421–1433.

Watson, J.G. and Chow, J.C. (2001). Source characterization of major emission sources in the Imperial and Mexicali Valleys along the US/Mexico border. *Sci. Total Environ.* 276: 33–47.

Watson, J.G., Chow, J.C. and Houck, J.E. (2001). $PM_{2.5}$ chemical source profiles for vehicle exhaust, vegetative burning, geological material, and coal burning in Northwestern Colorado during 1995. *Chemosphere* 43: 1141–1151.

Watson, J.G., Antony Chen, L.W., Chow, J.C., Doraiswamy, P. and Lowenthal, D.H. (2008). Source apportionment: Findings from the US supersites program. *J. Air Waste Manage. Assoc.* 58: 265–288.

Watson, J.G., Chow, J.C., Lowenthal, D.H., Chen, L.W.A., Wang, X. and Biscay, P. (2012). *Reformulation of $PM_{2.5}$ mass reconstruction assumptions for the San Joaquin Valley*, *Final Report*. Desert Research Institute, Reno, NV, USA.

Watson, J.G., Tropp, R.J., Kohl, S.D., Wang, X. and Chow, J.C. (2017). Filter processing and gravimetric analysis for suspended particulate matter samples. *Aerosol Sci. Eng.* 1: 93–105.

Weckwerth, G. (2001). Verification of traffic emitted aerosol components in the ambient air of Cologne (Germany). *Atmos. Environ*. 35: 5525–5536.

Wilson, J. G., Kingham, S., Pearce, J. and Sturman, A.P. (2005). A review of intraurban variations in particle air pollution: Implications for epidemiological research. *Atmos. Environ*. 39: 6444–6462.

Wongphatarakul, V., Friedlander, S.K. and Pinto, J.P. (1998). A comparative study of $PM_{2.5}$ ambient aerosol chemical databases. *Environ. Sci. Technol*. 32: 3926–3934.

Yang, H.H., Lai, S.O., Hsieh, L.T., Hsueh, H.J. and Chi, T.W. (2002). Profiles of PAH emission from steel and iron industries. *Chemosphere* 48: 1061–1074.

Yatkin, S. and Bayram, A. (2008). Determination of major natural and anthropogenic source profiles for particulate matter and trace elements in Izmir, Turkey. *Chemosphere* 71: 685–696.

Received for review, August 3, 2017
Revised, January 14, 2018
Accepted, February 4, 2018